6. SATELLITE, ORBIT AND THE VEGA LAUNCHER

6.1 LAUNCHER AND MISSION

The satellite will be launched directly into near-circular, near-equatorial orbit by a small / medium launcher such as Vega (baseline) or PSLV (backup). Both launchers have capability much in excess of a small spacecraft such as GG, and a dual launch might be taken into consideration (Figure 6-1).

The design launch altitude will be between 520 km and 600 km, according to the strategy discussed below. No orbit maintenance is planned, and the spacecraft altitude will be allowed to decay gently in time, with negligible impact on the satellite mission and operations.

A preliminary sequence of events is in Table 6-1. Once set up and initialized, the experiment will run in a regular way without any changes to either orbit or attitude. Given the near-equatorial orbit, the satellite will experience a regular once-per-orbit sequence of eclipses (35 minutes) and passes above the equatorial ground station of San Marco near Malindi, Kenya (about 10 minutes, with small variations depending on the selected altitude).

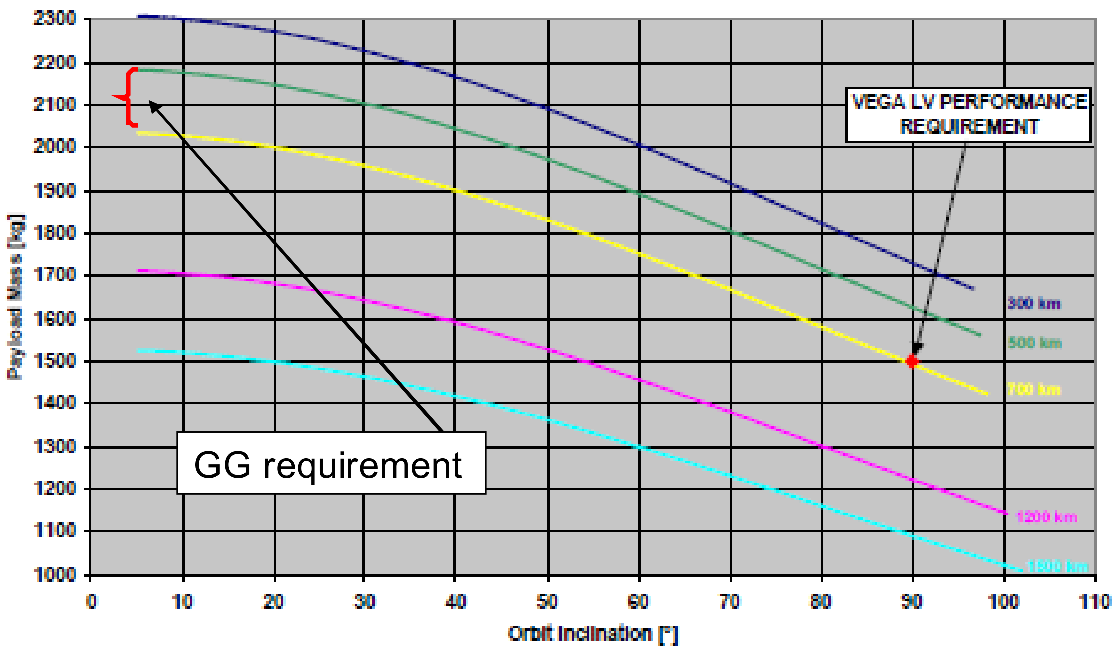

Figure 6-1: VEGA performance for circular orbits. The launcher requirement is 1500 kg in a 700-km altitude polar orbit. The lower limit to the orbit inclination is about 5°, and is set by the latitude of the Kourou launch site (5°N). For such a near-equatorial orbit, as required by GG, the VEGA performance is in excess of 2000 kg, much above the needed spacecraft mass.

Launch and Ascent Phase	
duration: ≈1 hour	3-axis stabilized release by the launcher satellite off on lift-off; activation of OBDH and RF by separation switch
Early Orbit Phase	
duration: ≈1 day	sun acquisition, rate damping and coarse spin attitude stabilization (autonomous) satellite acquisition by the EOP ground station network satellite health check
Satellite Commissioning	
duration: ≈1 week	satellite control handed over to the dedicated ground station subsystem commissioning satellite spin-up (semi-autonomous, assisted by the ground station)
Payload Switch-on and Calibration	
duration: ≈3 weeks	FEEP thruster switch on (pre-calculated thrust profile) Coarse thruster calibration Activation of electrostatic dampers common-mode sensing PGB unlocking Activation of common-mode sensing Activation of drag-free control Activation of spin rate control Test mass unlocking Test mass centering & alignment Fine test mass set-up / iteration
Scientific Mission	
duration: 2 years	Routine data collection Calibration
Scientific Mission Extension (optional)	
duration: until consumables are exhausted	Same sequence as in the Scientific Mission

Table 6-1: Sequence of events in the GG mission

The magnitude of the drag acceleration experienced by the satellite is a key to its performance, via the common-mode rejection ratio of the experiment and the drag-free control. As is well known, the scale height of the Earth's upper atmosphere (and thus the drag on low Earth orbit satellites) is very sensitive to the intensity of the short-wavelength solar radiation and the level of geomagnetic activity. Both parameters are function of epoch and are routinely forecast by a number of organizations, with sufficient accuracy for satellite lifetime and perturbation studies. In this study, we have used the 95% confidence level NASA forecast of the solar activity index F10.7, and of the daily global index of geomagnetic activity Ap, for the time period [2013, 2020], which encompasses atmosphere conditions ranging from near-solar maximum to solar minimum (see Figure 6-2).

In order to design the on-board systems independently of the epoch, a maximum acceleration threshold of 2×10^{-7} m/s^2 is specified, and the launch altitude is selected in such a way that the threshold will not be exceeded, in the time span of interest for the mission, at the 95% probability level. Given the downward trend of the solar flux from 2012 on, this criterion shows (Figure 6-3) that the mission design altitude needs to be >600 km if the launch occurs before 2015, and can be 550 km or lower if the launch occurs in 2016 or after. This range of variation of the altitude is of no consequence to either the launch mass or the scientific mission performance.

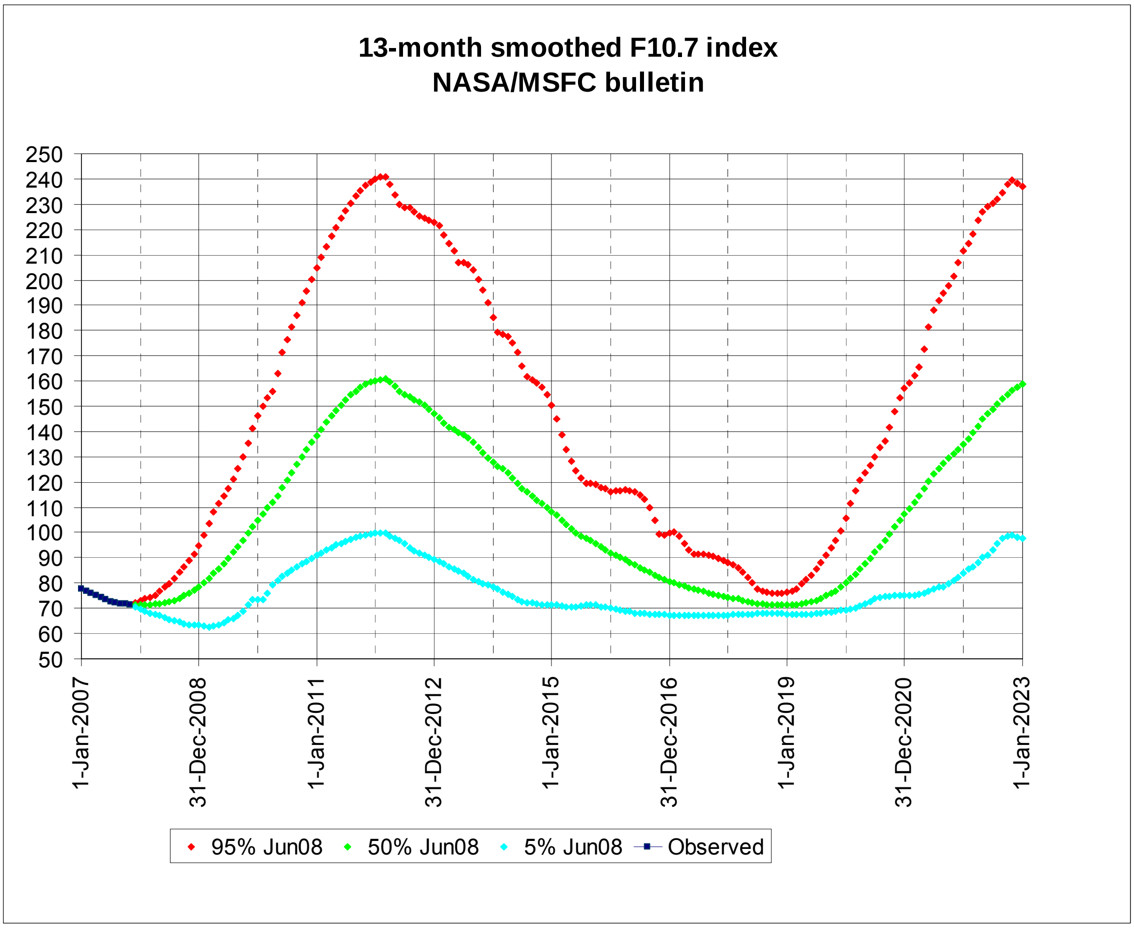

Figure 6-2: NASA forecast of F10.7 solar flux index [June 2008 NASA MSFC bulletin]

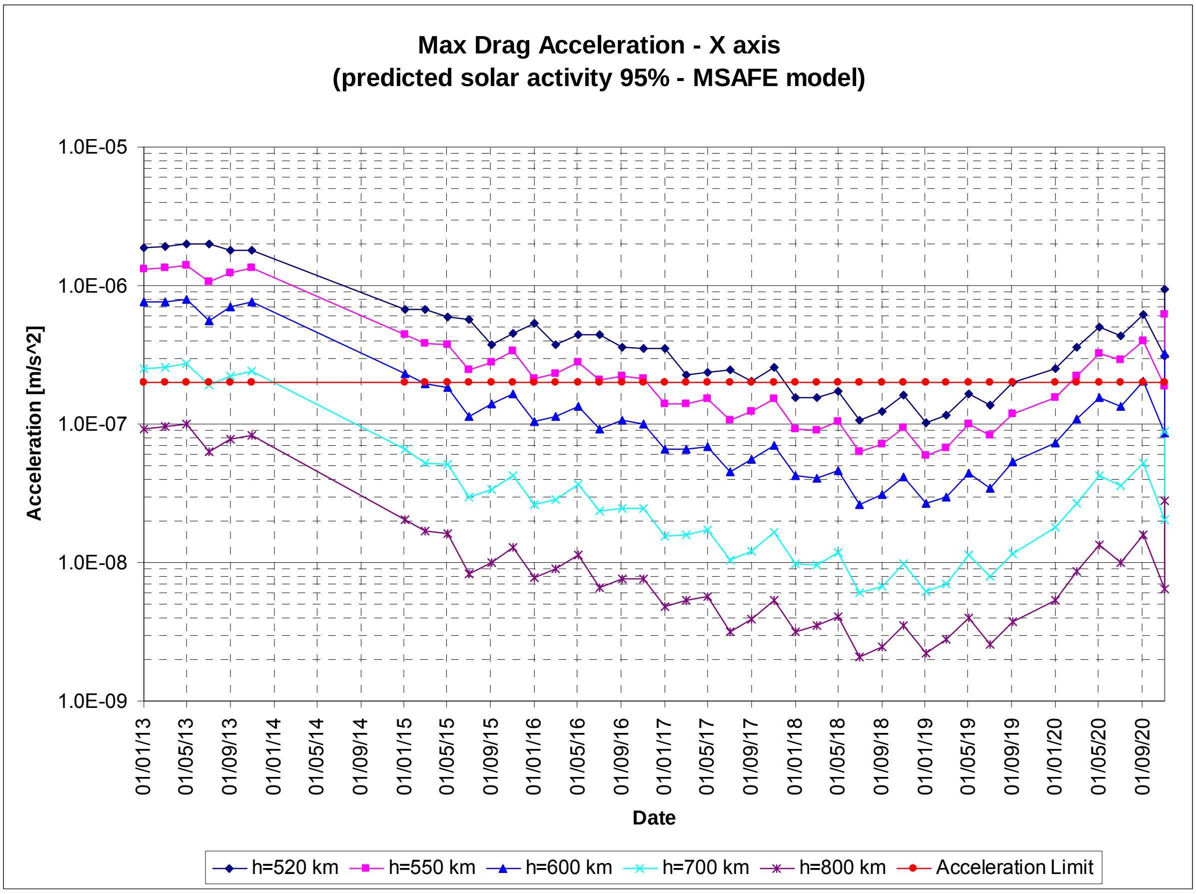

Figure 6-3: Parametric analysis of the drag acceleration. The atmospheric density is taken at the 95% probability level according to the NASA forecast of June 2008. The area-to-mass ratio is 0.0046 m²/kg. A maximum drag acceleration level < 2.0E-7 m/s² first becomes available at mean orbit altitude < 600 km in January 2015.

6.2 SATELLITE MECHANICAL CONFIGURATION

The cylindrical symmetry of the test masses and their enclosure, the Pico-Gravity Box, and the spin required to provide high frequency signal modulation, lead to a spacecraft of cylindrical symmetry, stabilized by rotation about the symmetry axis.

The main configuration requirements of the GG spacecraft are as follows.

- The GG experiment implies an ad-hoc configuration; reuse of an existing platform cannot be proposed. Conversely, many pieces of equipment may be inherited from the PRIMA complement.

- The spacecraft must be made compatible with the Vega launch vehicle (the previous design exercise was focused on Pegasus). In particular, the configuration shall fit the Vega fairing envelope, and the standard Vega 937 B adapter shall be used for launcher separation.

- The configuration shall allow easy integration of the PGB, with mounting/dismounting possible even during the last steps of the satellite integration.

- Low area-to-mass ratio is required ($\leq$ 0.005 m²/kg). The spacecraft shape and its mass distribution must have a degree of cylindrical symmetry. The spin axis must be a principal axis of inertia, with the following constraints
  - $J_{spin} > J_{trans}$
  - $\beta = (J_{spin} - J_{trans})/J_{trans} \sim 0.2 \div 0.3$.

The proposed solution is therefore a dedicated “spinning-top” structure supporting the PGB and equipment, plus two cylindrical solar panels; sensors and electric thrusters are mounted to a central belt, while the two S-band antennas, both fixed, are mounted on booms aligned with the spin axis.

The GG structural configuration is depicted in Figure 6-4. The external structure, completely enclosing the PGB laboratory, is made from CFRP, for minimum thermal distortions, and is made up of three parts:
- central cylinder with 1.4 m diameter, with thermal radiators cutouts;
- upper truncated cone, with the dismountable interface to the PGB suspension system;
- lower truncated cone, symmetrically placed, hosting the launcher interface ring.

The upper cone is removable to allow PGB integration. Equipment items are mounted internally to the central belt; thrusters and sensors are mounted externally. The solar array is made of two cylinders separated by a central belt for mounting equipment, including thrusters and sensors; this solution also allows a convenient distribution of thermal covers and radiators to achieve an efficient thermal control.

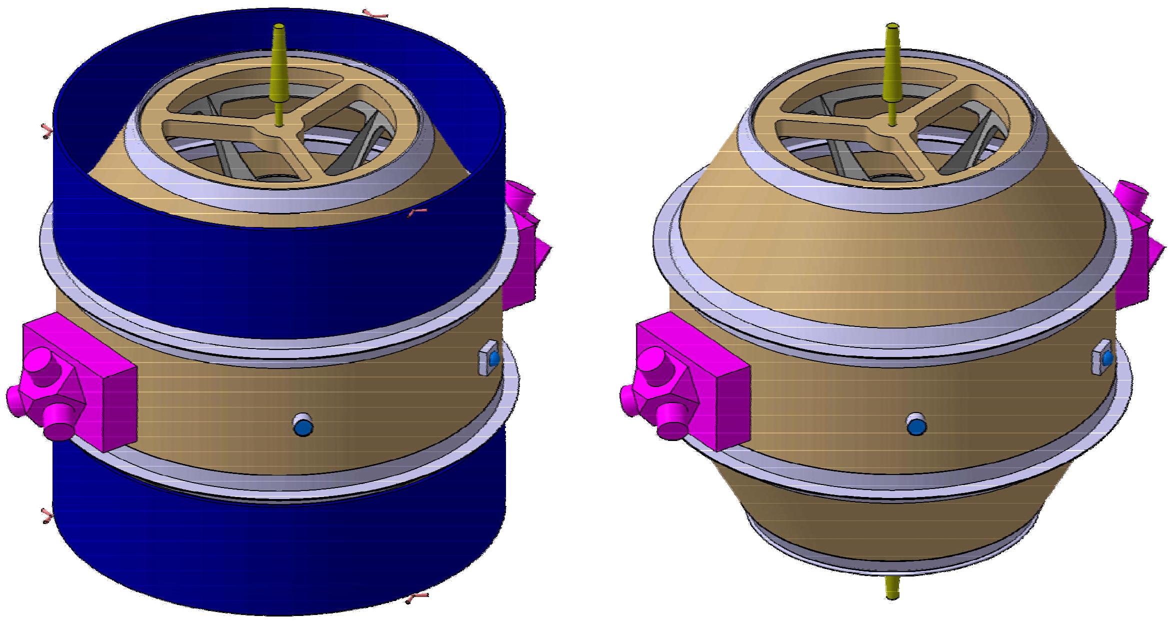

Figure 6-4: GG Spacecraft Configuration. Left: integrated configuration. Right: solar panels removed to show underlying structure.

The details of the configuration are listed below, from bottom to top, together with their component materials:

- interface ring with the launcher (7075 Al-alloy TBC);
- lower payload support cone (CFRP structure);
- lower circular plate with cut-outs, to support the lower LGA antenna;
- lower truncated cone (Al honeycomb with CFRP skins);
- lower cylindrical solar panel;
- central cylinder for mounting the equipment (Al honeycomb with Al skins);
- the equipment (see relevant s/s);
- upper truncated cone (Al honeycomb with CFRP skins);
- upper payload support cone (CFRP structure);
- upper circular plate with cut-outs, to support the upper LGA antenna;
- upper cylindrical solar panel;
- PGB assembly with the on-orbit suspension springs devices;
- two PGB launch-lock mechanism sets, released after launch;
- two antennas aligned with the spin axis, both fixed.

Figure 6-6 shows a 3D view of the satellite. The spacecraft body is about 1.45 m in outer diameter and about 1.42 m high. The experimental apparatus is accommodated in a nested arrangement inside the body, as shown in outline in the transparent view of Figure 6-6. As shown by Figure 6-5, there is plenty of mass and volume available for double launch with Vega, should it become possible.

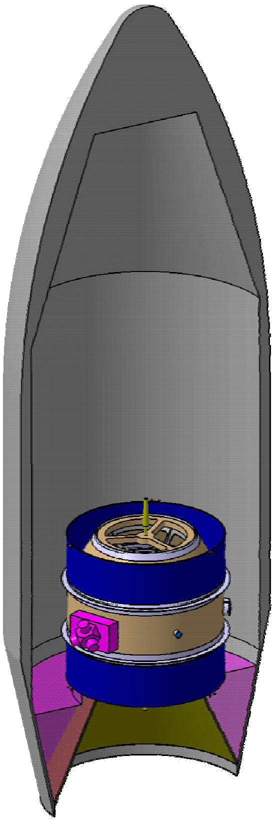

Figure 6-5: View of GG Spacecraft beneath Vega fairing

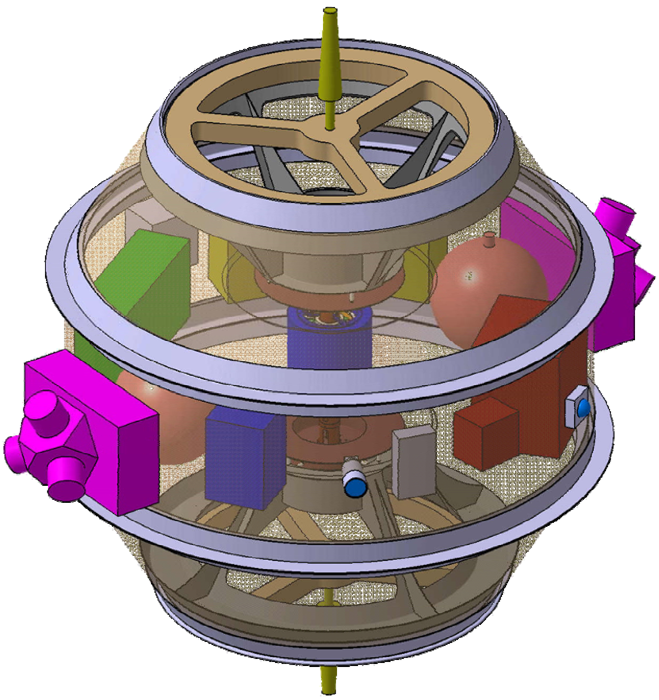

Figure 6-6: View of GG Spacecraft (transparent view)

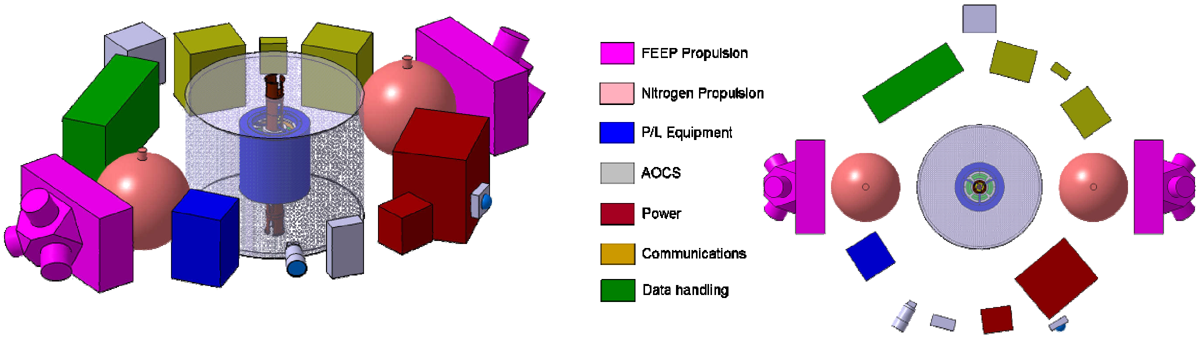

Figure 6-7: GG Spacecraft Preliminary Layout

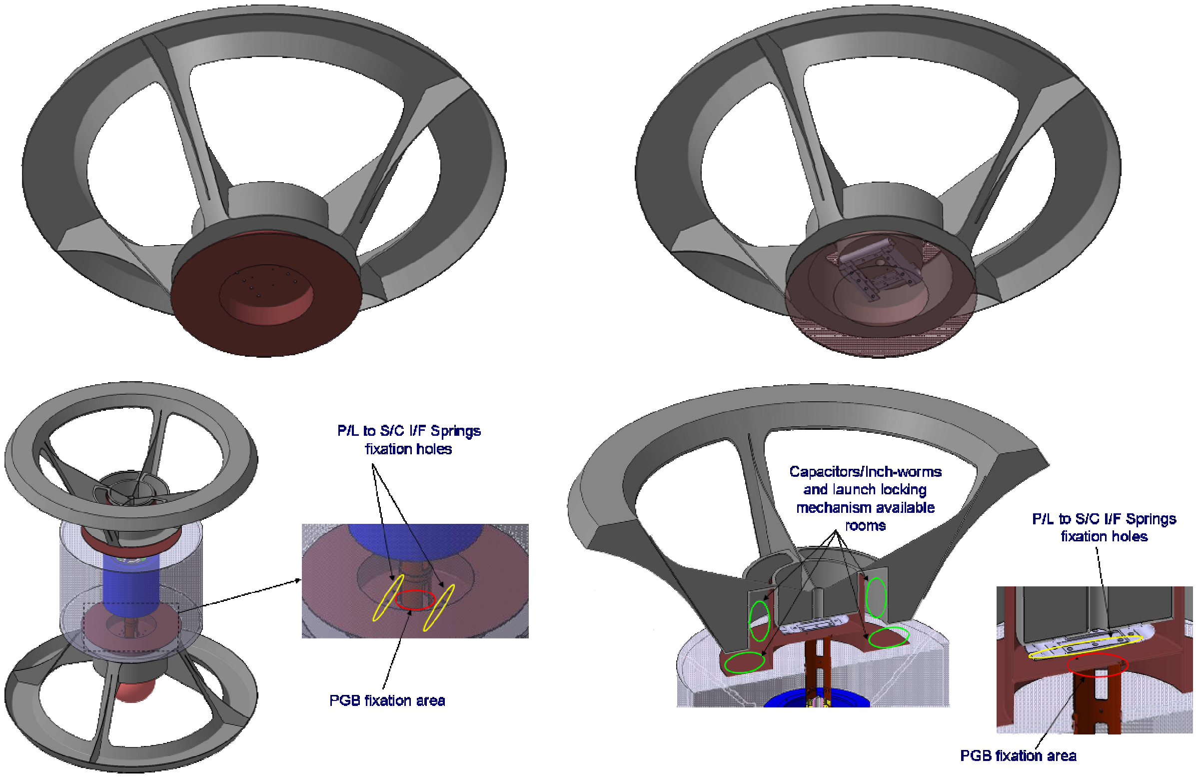

Figure 6-8: GG Experiment mechanical interface concept

Details about the equipment layout experiment mechanical interface concepts are provided in Figure 6-7 and Figure 6-8 respectively.

The current design maximizes the moment of inertia J_{spin} with respect to the symmetry axis, thereby providing passive spin stabilization around it, and meets the requirement with a $(J_{spin} - J_{trans})/J_{trans}$ ratio of ~ 0.3.

The spacecraft structure, similar to a spinning top, is exceptionally compact and stiff. Carbon fiber is used to the maximum extent to minimize thermal distortions. The central belt alone is composed of Aluminum honeycomb with aluminum skins for accommodation of the thermal radiators.

The total structural mass is 122.5 kg, including 20% subsystem margin. The launcher stiffness requirements are fulfilled with a satisfactory margin. The calculated first axial mode with the structure constrained at launch is 43.7 Hz (against > 20 Hz and < 45 Hz required by the launcher, see Figure 6-9). The first lateral mode is 26.2 Hz (>15 Hz required, see Figure 6-10).

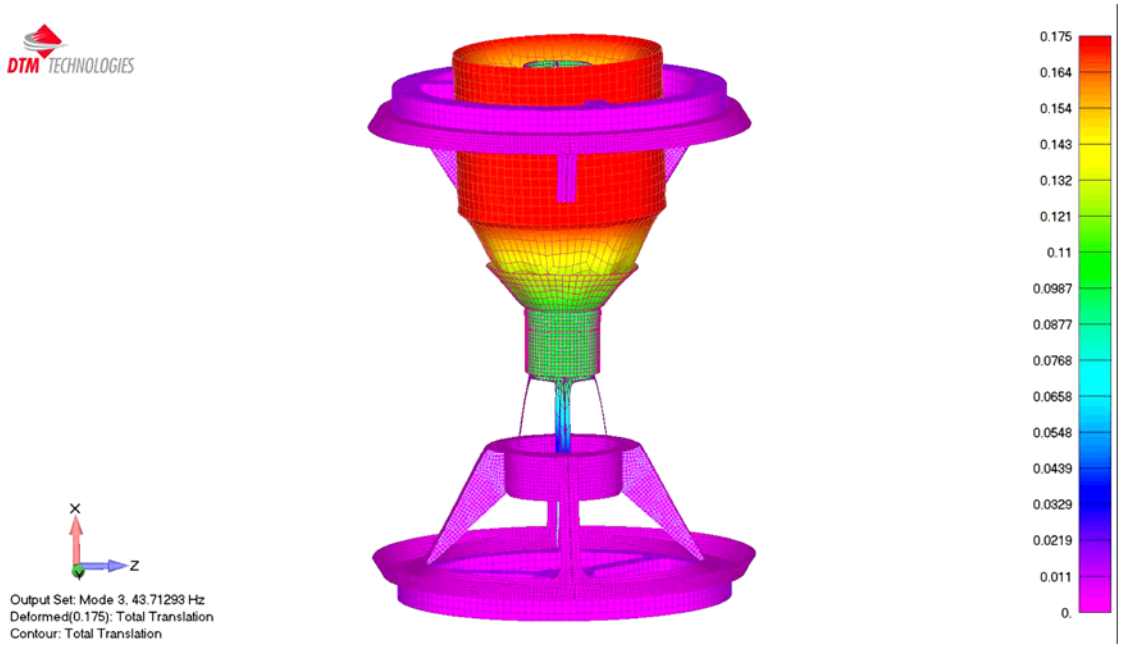

Figure 6-9: GG FEM Model first axial eigenfrequency (43.7 Hz, preliminary data)

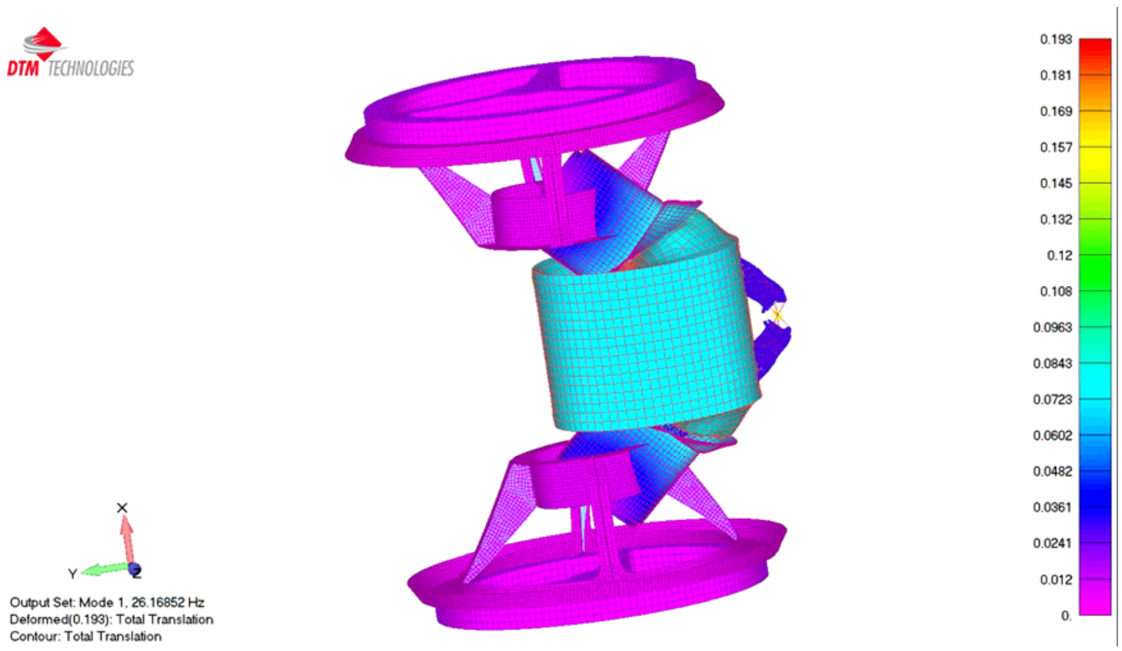

Figure 6-10: GG FEM Model first lateral eigenfrequency (26.2 Hz, preliminary data)

6.3 THERMAL DESIGN AND ANALYSIS

6.3.1 TCS REQUIREMENTS

The thermal requirements derive from the goal to maintain a thermal configuration able to perform the needed scientific measures. The high spin frequency value makes negligible the azimuthal temperature difference, while the axial effect shall be limited. Moreover it is important to maintain the temperature stable. The mechanical suspensions are sensitive to the temperature variation and this variation shall not degrade the common mode rejection of the mechanical suspension.

The following temperature requirements shall be met:

- test mass mean temperature stability better than 0.1°C/day;
- Axial temperature gradient at the level of the proof masses shall not exceed 1 °C/arm length;
- Temperature fluctuations in the proof masses shall not exceed 0.2 °C in 1 day;
- Linear temperature drift in the proof masses shall not exceed 0.2 °C/day.

As for the electronic units, the following temperature requirements were assumed:

- -20/+50 °C operating temperature;
- -30/+60 °C non operating temperature.

6.3.2 TCS DESCRIPTION

A classical passive approach plus heaters has been selected:

- The external side of the S/C will be covered by MLI blankets to counter the environment loads; painted radiators areas are distributed on the cylindrical structure following the footprint of the electronic boxes mounted inside the structural cylinder; solar arrays cells are placed on two dedicated cylindrical sections.
- The internal side of the S/C will be black-painted as much as possible where power is generated (internal cylindrical section and electronic boxes) in order to minimize temperature gradients, while a low-emissivity surface finish has been selected for both the external and the internal side of the PGB in order to radiatively decouple the payload from the remaining parts of the S/C.
- Electronics are mounted on the internal cylindrical structure via thermal fillers to increase the baseplates contact conductances; the PGB is conductively decoupled as much as possible from the remaining parts of the S/C, and the core of the payload is connected to the support structures via springs.
- The use of standard electrical heaters to trim or maintain the necessary temperature levels is under evaluation; if applied, this solution will be limited to the electronic boxes area, that is no heaters are envisaged inside the PGB enclosure in order to limit oscillation and temperature disturbances to the test masses.

The following thermal hardware is foreseen at this level of analysis.

MLI Blankets
Multi Layer Insulation blankets will be 20-layers ITO Kapton 3 mil with Dacron net spacers; the MLI will cover all the external surfaces except the radiators, solar cells and mechanical I/F with launch adapters. The S/C parts exposed to high heat input, i.e. plumes, will be shielded by 0.3 mil aluminised Kapton.
MLI blankets will also be used on the PGB cylinder, both on the external and the internal side.

Surface Finishes
Black paint Aeroglaze Z306 will be used for the internal side of the structural cylinder and as finish of the electronic boxes.
All the remaining parts of the internal environments will have a low-emissivity finish, not exceeding 0.05.
The external radiator areas will be covered with silvered Teflon tape.

Thermal fillers
Sigraflex-F will be used to increase thermal coupling between equipments and the mounting surfaces (brackets or structural panels).

6.3.3 MATHEMATICAL MODEL DESCRIPTION

Geometrical Mathematical Model (GMM)

Esarad 6.2 has been used to build up the Geometrical Mathematical model and to run the radiative analysis. The GMM includes all the main structural elements, the payload components, and the equipments both inside and outside the S/C:

- Structural main cylinder, cones, flanges and payload support structures
- Internal electronic boxes
- PGB protective cylinder, I/F flanges and springs
- Payload internals: Mass 1, Mass2, Capacitive Plates, and support cylinders brackets and flanges
- External MLI blankets, sensors, antennas and Solar Arrays.

The following figures depict the modeled elements.

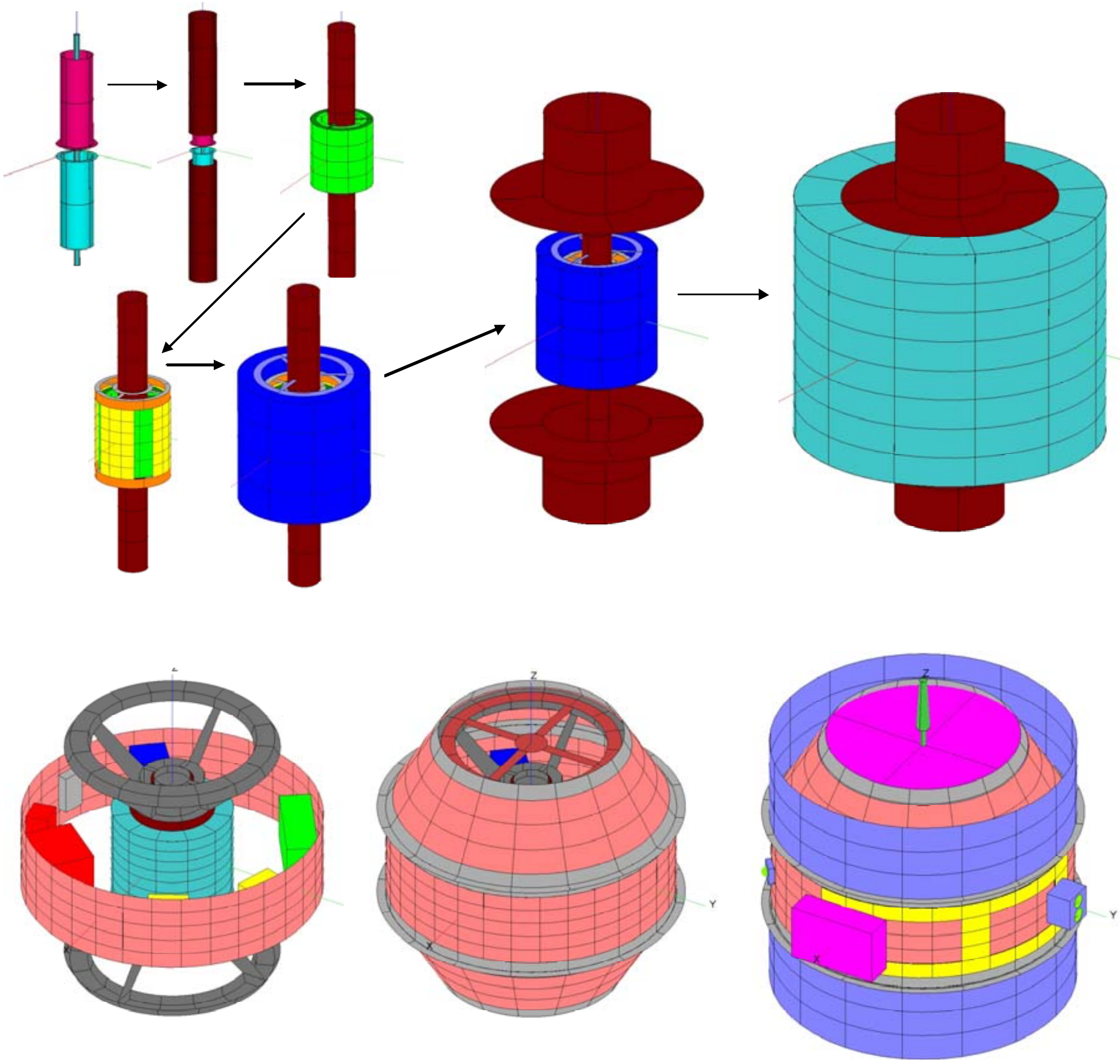

Figure 6.11: Overall GG Geometrical Mathematical Model component breakdown

The radiator areas have been positioned only on the outer cylindrical part of the structure, and in general follow the arrangement of the internal boxes. Radiator areas implemented in the GMM are listed in Table 6.1.

Unit	Radiator area [m^2]
Battery	0.067
PCE	0.122
CDMU	0.234
TRANSP 1	0.100
TRANSP 2	0.100
PCU	0.300
Tot Radiative area [m^2]	**0.923**

Table 6-2: Radiator areas

The GMM is made of 2090 nodes and 509804 radiative conductors are calculated as output. A summary of the thermo-optical properties and the main orbit data is given in the following two tables.

Thermo-Optical properties			
Surface finish	ε	α BOL	α EOL
MLI ITO Kapton	0.77	0.30	0.43
MLI Aluminised Kapton	0.05	0.14	0.14
Black paint Z306	0.88	0.96	0.96
Silvered Teflon tape	0.75	0.14	0.30
Bare aluminium	0.05	0.21	0.21
Solar Array Cell Side	0.82	0.75	0.75
Solar Array Back Side	0.71	0.51	0.51

Table 6-3: Thermo-optical properties

Orbit and Attitude data		
Orbit	Orbit case	EOL
	Earth-Sun distance	149.5979 E06 Km
	Sun temperature	5770 K
	Orbit eccentricity	0
	Orbital altitude	520 Km
	Orbital period	5699.35 s
	Earth albedo factor	0.35
	Earth temperature	263 K
Attitude	Attitude	+Z normal to orbit spin axis
	Number of orbital positions	10
	Spin rate	720 deg/s
	Spin results averaged over	12 positions

Table 6-4: Orbit and Attitude properties

Thermal Mathematical Model (TMM)

The Thermal Mathematical Model has been written to run in Esatan 10.2 code. The linear thermal network is made by 4309 conductors. The material properties used in the TMM (thermal conductivity, heat capacity, mass density) are listed in the Table 6-5 and Table 6-6.

A very conservative approach has been used for the units power dissipation evaluation. For each orbit, the maximum value of power dissipation has been considered when the S/C is exposed to the Sun flux, while the minimum value has been taken into account during the eclipse phase. A summary of the figures used is given in Table 6-7.

The electronic units are placed on the internal side of the main structural cylinder; in the TMM, units are coupled directly to the cylinder H/C. Brackets and mounting structures have not been taken into account at this level of analysis.

Element	Material	Thermal conductivity	Heat capacity	Density	Comments
Structural panels: cylinder, cones, solar arrays	Honeycomb	KXY=10.8 W/K KZ=1.8 W/m2/K	900 J/kg/K	2.5 kg/m2	Al skin 2*0.4 mm Al core 15 mm
Structure: Rings, flanges, PGB I/F, Payload support structures, S/C launcher I/F Payload: TM1, TM2, Capacitive Plates brackets, flanges, support cylinders	Al 7075	150 W/K	900 J/kg/K	2700 Kg/m3	
Test Mass 1	Pb	35 W/K	129 J/kg/K	11340 Kg/m3	
Test Mass 2	Al 7075 (1)	150 W/K	900 J/kg/K	2700 Kg/m3	
Capacitive Plates	Cu	390 W/K	380 J/kg/K	8920 Kg/m3	
Propellant tanks	Ti	10 W/K	520 J/kg/K	4500 Kg/m3	
MLI blankets	20-lay Kapton	temperature dependent (see Table 6.6)	0	0	

(1) In a conservative approach, only the Aluminium box containing the Polypropylene Mass 2 has been considered.

Table 6-5: Materials thermal properties

Structure	Element	Material	Thickness [mm]
Payload inner support cylinders	cylinders	Al 7075	1.609
	cylinders flanges	Al 7075	3.0
Payload outer support cylinders	cylinders	Al 7075	1.565
Test Mass 1 support structure	circular flange	Al 7075	5.0
	brackets	Al 7075	6.5
	mass cylinder	Al 7075	23.1
Test Mass 2 support structure	circular flange	Al 7075	3.0
	brackets	Al 7075	3.0 - 4.5
	mass cylinder	Al 7075	37.8
Capacitive Plates support structure	circular flange	Al 7075	2.0 – 11.04.0
	brackets	Al 7075	4.0
	plates supports	Al 7075	6.0
	plates	Al 7075	2.0
PGB	I/F structure	Al 7075	2.5
	protective cylinder (1)	Al 7075	3.0
H/C structural supports	cylinder ring	Al 7075	2.5
	cylinder flange	Al 7075	5.0
	cone flanges	Al 7075	2.5
	upper/lower platforms	Al 7075	60.0

(1) Two Protective Cylinder configurations have been analysed: one made of Aluminium (shown in this table) and one made of MLI (without any support structure)

Table 6-6: Structure panels thermal conductivity

Unit	Power in Sun [W]	Power in Eclipse [W]	Remarks
BATTERY	11	0	
SRS	1	0	
CPE	23	0	
CDMU	45	14.4	
TRSP2	20	6	TX (10 min/orb) = 20W RX = 6W
RFDN	0	0	
TRSP1	6	6	
PCU	55	14	
EPSA+PPCU+NEUTRAL	30	0	
ECE (1)	12	12	
Tot without ECE	191	40.4	
Tot with ECE	203	52.4	

(1) ECE has been considered only in one analysis case, see Results chapter for details

Table 6-7: Units power dissipations

6.3.4 Analysis results

Esatan 10.2 was used for a first series of transient analyses. The purpose is to gain sensitivity over the driving parameters of the models and to explore the response of the payload to variations of the boundary conditions.

At this level of the analysis, a hot orbital environment (direct Solar flux peak 435 W/m^2, albedo factor 0.35, Earth temperature 263K), and a conservative power dissipation profile during the orbits were assumed.

A summary of the analysis cases is given in Table 6-8. A detailed description is given of Case 1 (baseline); the results of other cases are summarized in the conclusions. The results of analysis are given always for 20 orbits after 180 orbits of stabilization.

Case ID	Description	Remarks
1	EOL environment and thermo-optical properties PGB with Aluminum finish (ε=0.05) Standard power dissipation profiles No heater power applied	Baseline case
2	EOL environment and thermo-optical properties PGB with Black Paint finish (ε=0.88) Standard power dissipation profiles No heater power applied	Evaluation of radiative environment of the internal payload
3	EOL environment and thermo-optical properties PGB with Aluminum finish (ε=0.05) Standard power dissipation profiles, but TRSP2 in TX (20W) only for 10min/orbit instead of the entire sunlit phase No heater power applied	Evaluation of power dissipation profiles of electronic units
4	EOL environment and thermo-optical properties PGB with Aluminum finish (ε=0.05) Standard power dissipation profiles + ECE power inside the PGB (12W) No heater power applied	Evaluation of power dissipation on the internal payload
5	EOL environment and thermo-optical properties PGB with Aluminum finish (ε=0.05) Standard power dissipation profiles PGB with of MLI No heater power applied	Evaluation of insulation of the internal payload

Table 6-8: Analysis cases for sensitivity

Results of Case 1

As baseline configuration, all the internal S/C environment is considered black painted (ε=0.88), except the PGB interior, which has a bare aluminum finish (ε=0.05) for all the items contained; the PGB protective cylinder is made of aluminum (ε=0.05 both for the external and the internal side).

Test Mass 1, Test Mass 2 and the Capacitance Plates nodes show a temperature drift, but both the spatial (ΔT<1°C/arm length) and the temporal (ΔT<0.2°/day) temperature requirements are met. See Figure 6-11 to 6-13.

All the spacecraft units remain within limits even if no heater power is applied:

time	BATTERY	SRS	CPE	CDMU	TRSP2	RFDN	TRSP1	PCU
T MIN	*-3.99*	*-6.34*	*2.01*	*4.62*	*10.84*	*-6.02*	*-1.21*	*7.99*
T MAX	*4.38*	*-3.35*	*7.40*	*7.93*	*14.08*	*-3.50*	*-0.42*	*11.14*

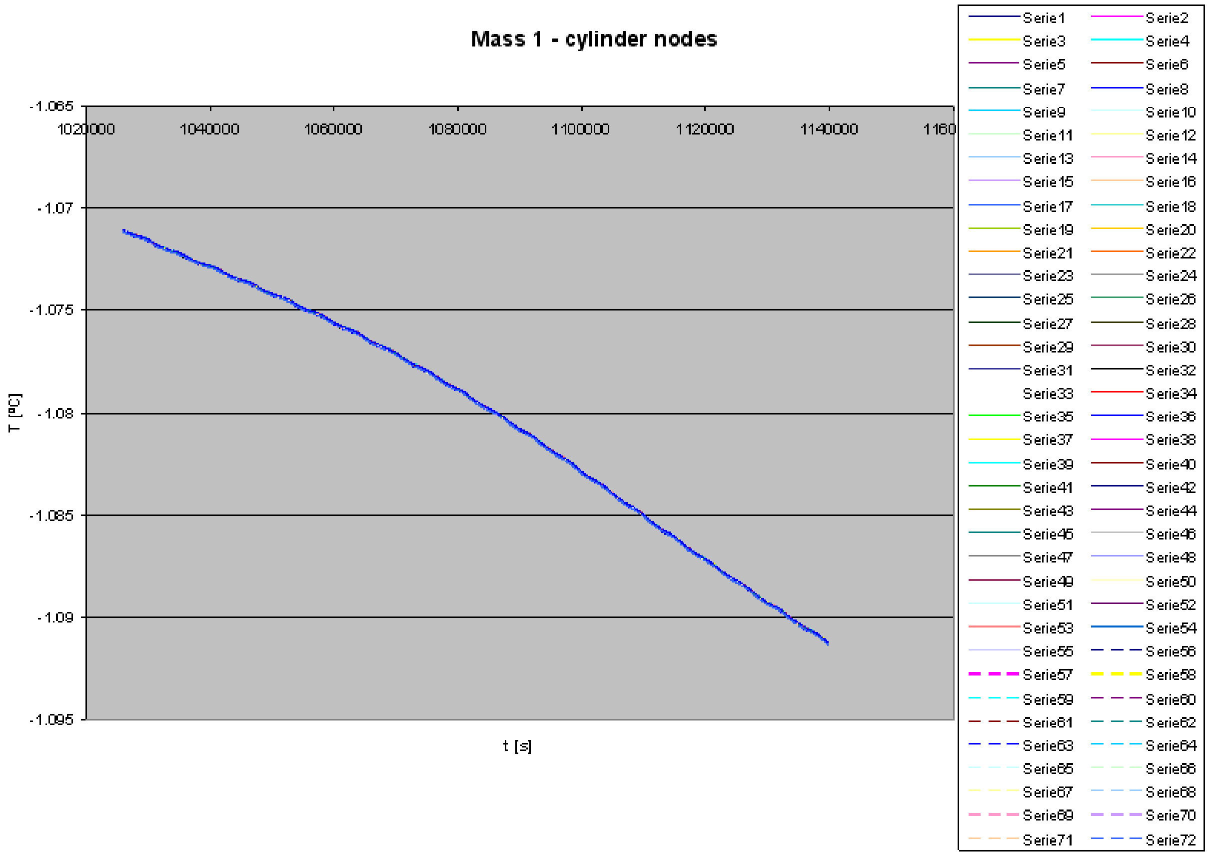

Figure 6-11: Thermal analysis of Case 1: Test mass 1 thermal nodes

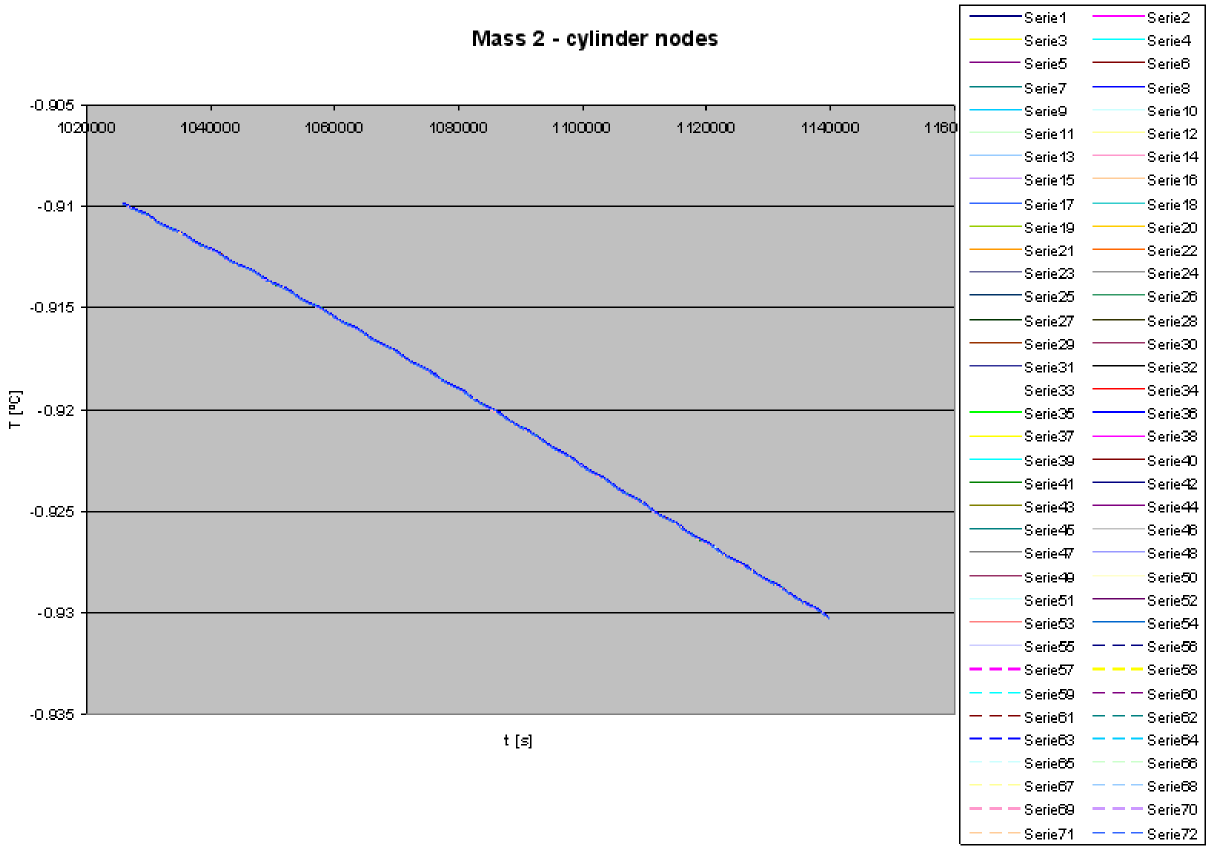

Figure 6-12: Thermal analysis of Case 1: Test mass 2 thermal nodes

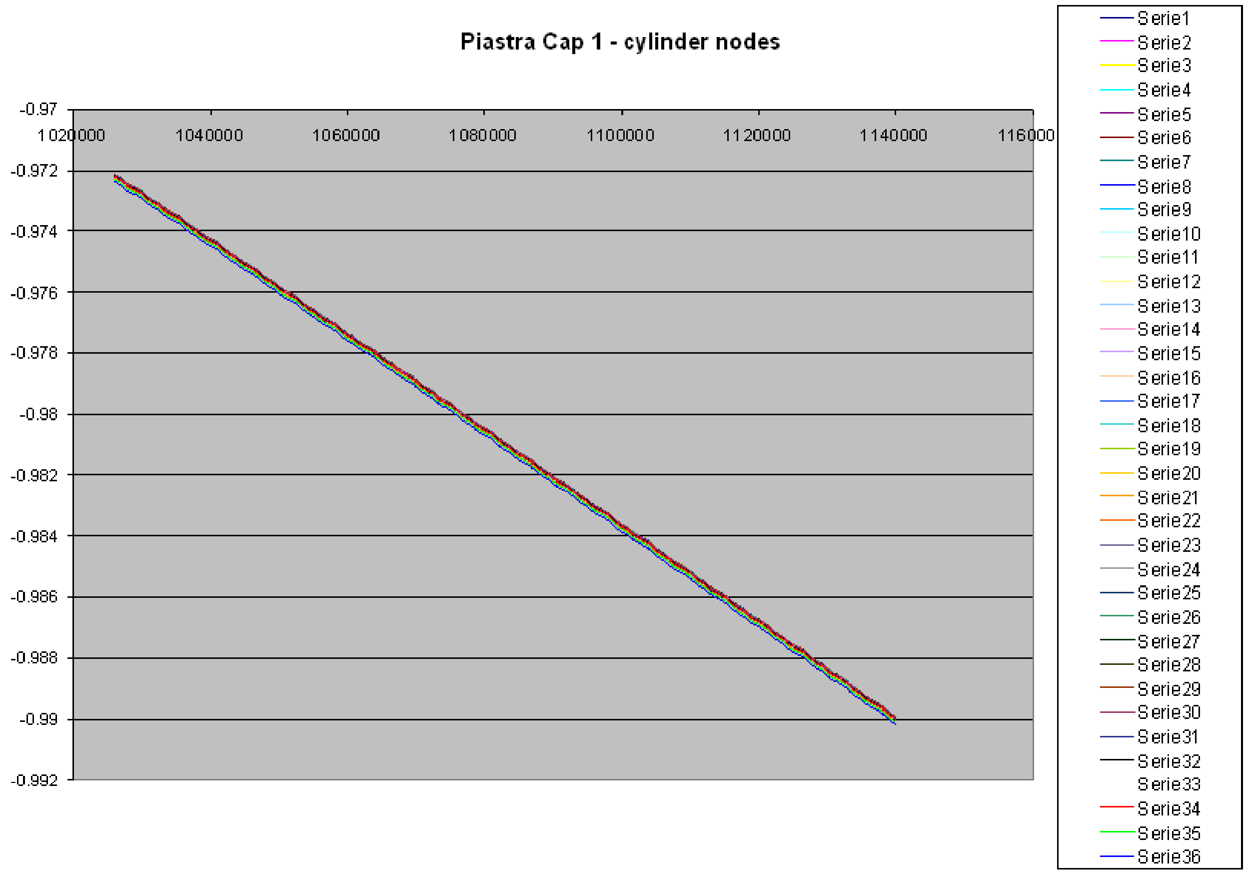

Figure 6-13: Thermal analysis of Case 1: capacitance plate 1 thermal nodes

6.3.5 CONCLUSIONS

After the described preliminary analysis campaign, the following remarks are made.

A number of assumptions have been introduced in the mathematical models:

- For Test Mass 2 body aluminum has been considered as material in the TMM; the foreseen Polypropylene mass contained inside an aluminum body will be implemented in the TMM as soon as this configuration will be confirmed;
- Conservative power dissipation profiles have been considered: maximum dissipation power is considered while the S/C is in sunlight, while minimum dissipation power is considered while the S/C is in eclipse, leading to a wide variation in the internal produced heat for each orbit (191W in sunlight and 40.4W in eclipse in the case without ECE dissipation);
- Calculations take into account 180 orbits for stabilization and 20 orbits for output;
- The PGB support structure is made of aluminum, conductively connected to the satellite structure by two laminar CuBe alloy springs sets only (GL = 0.0021 W/K each).

These assumptions need to be reviewed and harmonized with the final payload design.

At the current level of analysis, no need to use electrical heaters is foreseen.

Use of black paint inside the PGB makes the payload elements more sensitive to the external disturbances; on the other hand, black paint allows the internal components of the payload to approach the equilibrium conditions faster.

The design of the protective cylinder seems adequate even if simulated by an aluminum cylinder (conservative approach).

Power dissipation inside the PGB should be minimized, as it affects the performance both in terms of space (temperature gradients between two points of the test masses) and in terms of time (temperature drift in the test masses).

Due to the high decoupling of the internal payload from the rest of the S/C, long times are needed to approach the equilibrium temperatures, even if the temperature variations during this time are within the requirements. A more detailed analysis is mandatory to estimate the time constant of the system.

MLI, structural elements and solar panel temperatures show normal temperature levels and are of no concern.

6.4 ELECTRICAL AND ELECTRONIC DESIGN

Figure 6-14 shows the GG avionic system architecture, comprising both payload electronics units and service module units.

The Payload Electronics is composed by two major subsystems:

- PGB Control and Processing Electronics (CPE)
- Experiment Control Electronics (ECE).

The PGB Control and Processing Electronics, located on the spacecraft platform, manages PGB motion control (whirl sensing, whirl damping) and the processing of all signals coming from the test masses (motion control and EP sensing). Moreover, the CPE performs:

- TC reception from spacecraft and decoding;
- execution of payload timelines and commands;
- Science data collection, compression and formatting;
- Formatting of TM packets and their transmission to the spacecraft.

The Experiment Control Electronics, housed inside the PGB, communicates with the CPE via an optical link. It performs readout of the EP chain and, under control by the CPE processor, manages locally the whirl sensing and damper activation.

The service module electrical architecture includes:

- On Board Data Handling
- Electrical Power System including PCDU, solar array and battery.

6.4.1 ON-BOARD DATA HANDLING

The GG on-board data handling system will be based on a single CDMU, derived from the standard LEONARDO unit, developed via the ASI PRIMA program and based on an ERC32 CPU. A dedicated CPU board, equipped with LEON2FT processor, based on a standard ASIC, is under qualification by TAS-I. If necessary this board could replace the ERC processor board.

The CDMU acts as the central communication node between the Spacecraft and the active Ground Station, distributing or executing commands received from ground and collecting, formatting and transmitting the satellite telemetry.

The CDMU provides: telecommand acquisition, decoding, validation and distribution; scientific and HK data acquisition and storage; distribution of time reference signals for the Central Reference Time generator and synchronization with the local timers of the other processors; autonomy supervision and management.

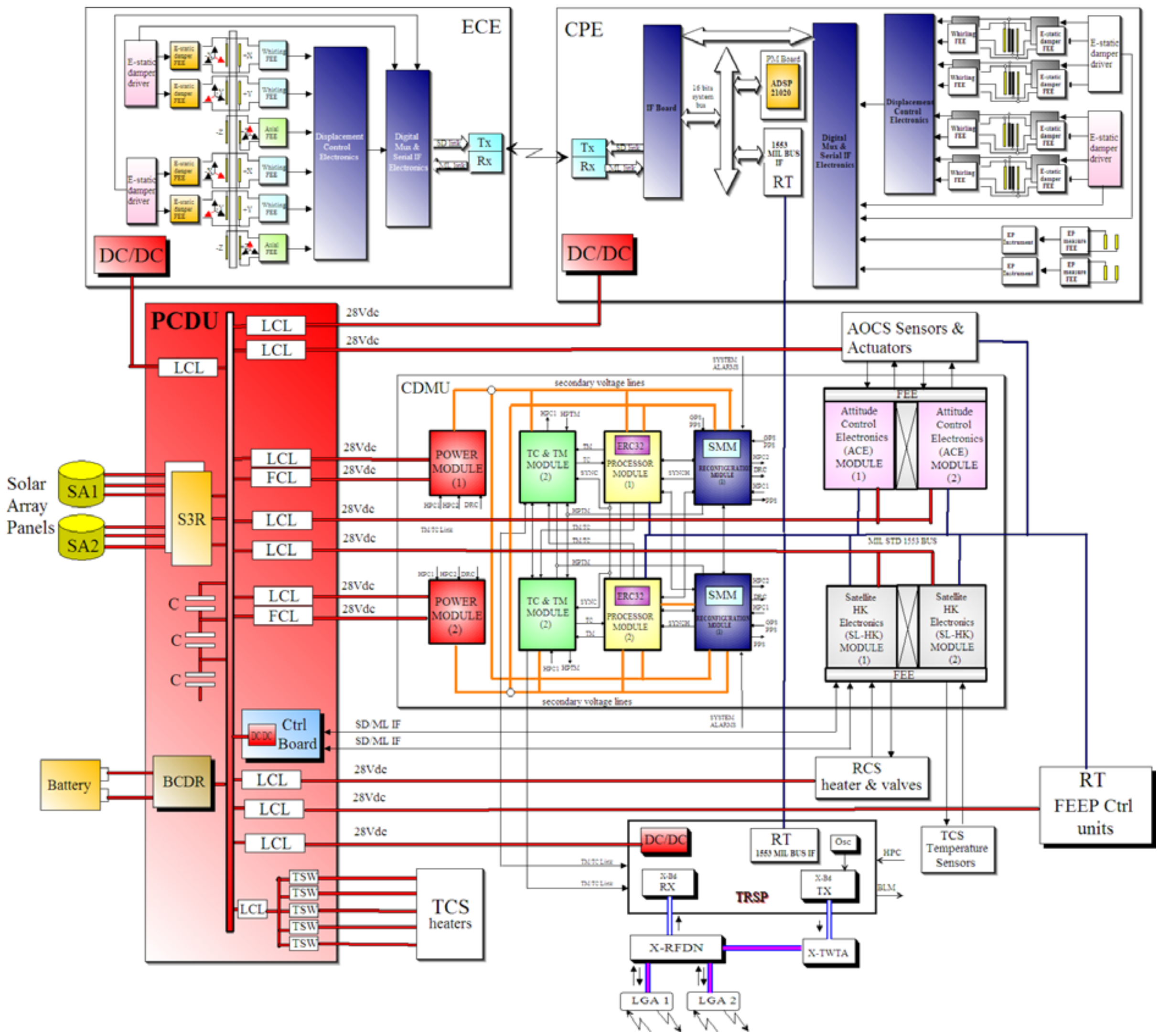

Figure 6-14: GG avionic architecture block diagram.

Within the centralized CDMU computer, all the application software will be executed, including the software implementing the AOCS and drag free control algorithms.

The CDMU provides a number of discrete telecommand lines for reconfiguration purposes. It provides condition inputs for discrete telemetry lines which will be used for housekeeping, to acquire status monitors and temperatures from the Thermal Control sensors. Power to Thermal Control heaters is provided by the PCDU, under CDMU commands received on the 1553 bus.

Decoding and validation of telecommands uplinked from ground is performed by the TC decoder embedded in the CDMU. A set of High Priority Commands is available to command directly the end users from the decoders, by-passing any on board processor. These commands are used for time critical functions such as activation/deactivation of units, on board computers re-initialization, back-up initiation of post-separation sequences.

The CDMU includes a Reconfiguration Module, functionally independent from the Processor Module and the On Board Software, capable of processing some alarm signals via dedicated links and of commanding directly the end users via the High Priority Commands.

Moreover, the CDMU will be equipped with internal power supply dedicated boards, based on standard FPGAs (Actel RTSX), to drive all the required mechanisms and actuators. Finally, the box will implement an acquisition module dedicated the internal HK and the conditioning of the sensors and acquisition needed to control the mechanisms.

The GG CDMU will be based on dedicated tailoring of a TAS-I heritage architecture (Figure 6-15), based on the experience gained with the development of many control units.

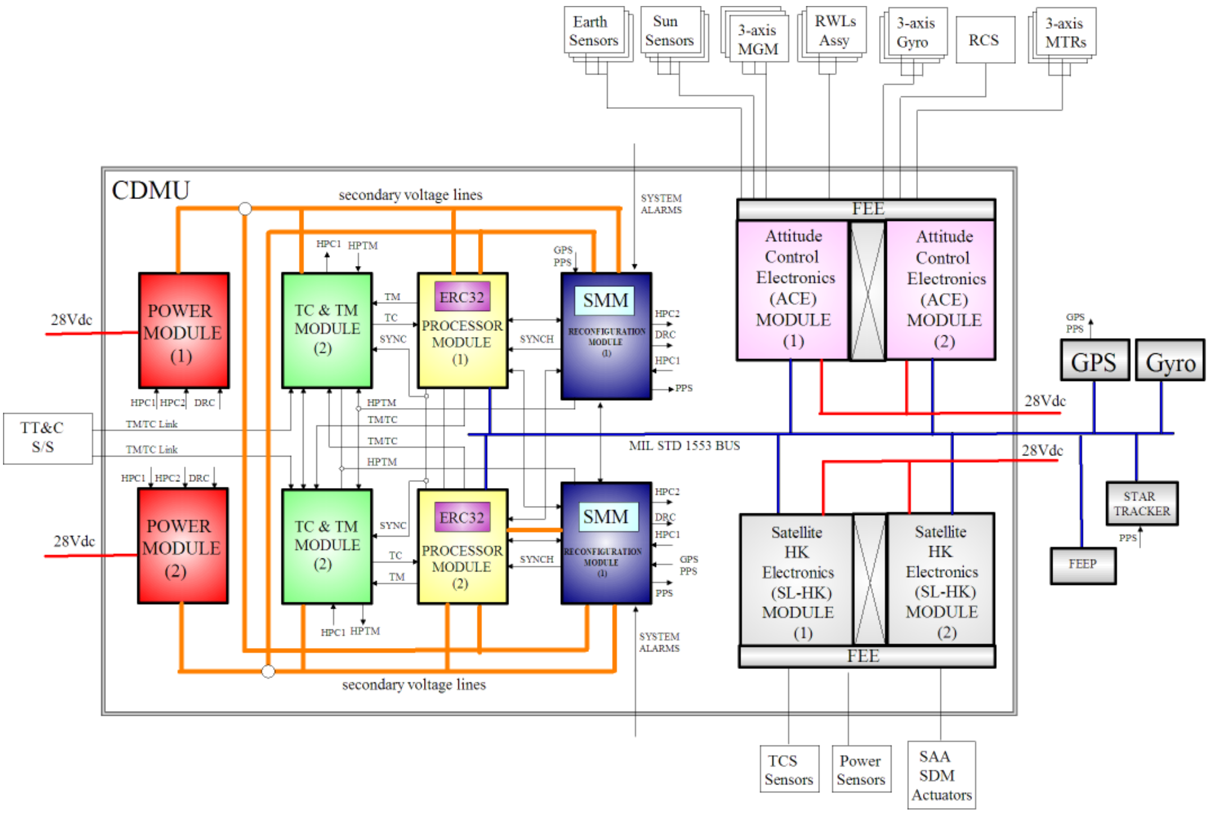

Figure 6-15: Functional block diagram of a generic CDMU based on TAS-I heritage.

6.4.2 ELECTRICAL POWER SYSTEM

The Electrical Power System (EPS) is implemented by a dedicated Power Distribution and Control Unit (PCDU), plus power generators and a battery.

On the basis of the power budget, the EPS is required to provide around 520W for both payload and S/C equipment, constantly along the whole mission duration of 2 years.

A fully regulated 28V power bus was adopted, compliant with the ESA power standard, under the assumption that the payload electronics only allow operation in a limited range of bus voltage variation. This design also increases the power conversion efficiency in the EPS system and reduces EMC noise.

For the Solar Array power regulation, either an S3R regulator or an MPPT regulator could be considered. An S3R regulator design is preliminarily assumed, considering its simple operation (constant attitude to the sun), the simplicity and robustness of the design and the good flight heritage. By regulating the number of SA sections connected to the bus, the bus is controlled to be at fixed voltage value.

In series to the S3R regulator there are two buck DC/DC converters, providing the required 28 V power bus voltage conversion and regulation using a majority voted Main Error Amplifier (MEA).

Taking into account the regulated bus topology, a single BCDR module can be implemented, consisting of two power regulators, a Battery Change Regulator (BCR) and a Battery Discharge Regulator (BDR).

<u>PCDU configuration</u>

The PCDU provides the following functions:
- it controls the electrical power generated by the solar array;
- conditions the energy stored in the battery when required;
- controls, monitors and maintains the health of the EPS;
- distributes power to the scientific instruments and spacecraft equipment;
- protects the power bus from external faults and prevents failure propagation;
- provides heater switching control in response to commands;
- interfaces for AIV and Launch support EGSE.

The proposed modular PCDU, derived from the ASI PRIMA PCDU (SMU) design, has the following features.
- 28V regulated Power Bus
- Up to 700 W distributed power
- At least 4 I/F with independent Solar Array sections and 1 Li-Ion Battery
- S3R concept
- SD/ML TM/TC I/F

- Outputs:
  - 12 FCL (Fold-back Current Limiters)
  - 24 LCL (Latching Current Limiters)
  - 60 heater lines.

The PCDU will include the following main boards:
- Array Power Regulation modules;
- Battery charge/discharge regulator modules;
- Command and Monitoring modules;
- Back Plane;
- Heater Distribution module.

Battery configuration

The battery provides a store for the excess solar array energy, and a source of energy whenever there is insufficient power from the array (e.g. during launch, transient power demands and eclipse periods). The selected equatorial orbit leads to eclipse on every orbit with duration of about 36 minutes over a period of 95 minutes.

The Sony 18650HC Li-Ion cell technology is considered for the battery. The battery sizing case is energy supply of the satellite during the entire LEOP phase assuming a power load of 171 W for 120 minutes. Considering a battery with 27 Ah capacity (18px7s), initial State of Charge (SoC) of 98% and 1 failed string, the final SoC after the LEOP will be 69.7 % with the voltage of the battery at 26.74V.

The battery discharge and charge profiles, and the expected SoC degradation at end of Life (EoL) were calculated assuming maximum Depth of Discharge (DoD) of 30%. The resulting SoC degradation at EoL is 13 % with 11,100 charge/discharge cycles over the expected mission lifetime.

The assumed efficiencies are 94% (BDR) and 96% (BCR). Summarizing, the calculated battery characteristics under the assumptions listed above are:
- Capacity of 27 Ah
- Energy 633.15 Wh @3.35 V
- Configuration: 18p7s
- Mass: 6.35 kg (including 20% maturity margin)
- Dimensions: 200mm x 120mm x120mm.

Solar array configuration

The Solar Array consists of two cylindrical surfaces equipped with RWE 3G-ID2L/150-8040 cells. They will be used to generate the power necessary to supply the S/C and P/L electronic units and heaters during the sunlit period, while spinning at 1 Hz.

Cells shall be organized in strings to achieve the required voltage, but as the current delivered by each string is limited by the least illuminated cell, it is necessary to grant constant illumination over the entire string in order to both optimize the power conversion efficiency and minimize cell degradation. Cells shall be stacked vertically on the cylinder surface to form strings. The length of a single cell determines how many such stripes can be disposed while the height limits the number of cells per string.

As first approximation the collected solar flux of the cylindrical surface can be approximated by its projection:

$$\eta_{area} = \frac{Projectedsurface}{HalfLateralSurface} = \frac{2Rh}{\pi Rh} = 2/\pi \cong 0.637$$

Unfortunately this approximation is not conservative as below specific incidence angles the conversion efficiency degrades more than the cosine projection and becomes negligible around 85°. The relative power of solar cells has therefore been calculated according to the following empirical formulation:

$$\begin{array}{ll} \gamma < 50^\circ & P/P_o = \cos(\gamma) \\ 50^\circ \le \gamma < 85^\circ & P/P_o = 1.149 - 5.99e-3 \cdot \gamma - 8.65e-5 \cdot \gamma^2 \\ \gamma \ge 85^\circ & P = 0 \end{array}$$

The γ angles have been calculated for every string exposed to the Sun on the cylindrical surface. The collected and usable flux on the exposed cells area results in the order of 780W/m^2, which, including a packing factor of 0.9, translates into an area exploitation efficiency of η_{area}=0.48.

For the S3R an equivalent efficiency of 95 % is considered. Given the available surfaces and the cell characteristics, the following SA configuration is found: 15 cells per string, 38 strings per cylinder, 2 cylinders. This SA configuration requires a total used area of 3.6 m² to supply a maximum power load of 519 W.

6.5 TELECOMMUNICATIONS

An S-Band architecture derived from the PRIMA platform is proposed for the Galileo Galilei TT&C. The architecture, shown below, consists of:

- 2 transponders with low output power (23 dBm, i.e., 200 mW) and diplexer embedded;
- RFDN miscellanea in coaxial technology:
  - 3-dB hybrid coupler
  - Connection cables;
- 2 LGAs with circular polarization and hemispherical coverage (gain = -3 dBi at ±90° boresight offset angle)

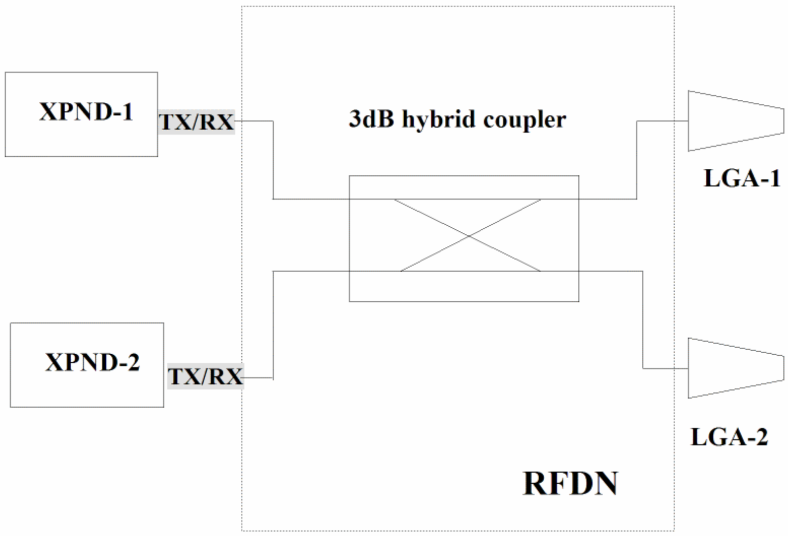

Figure 6-16: GG TT&C block diagram

The telemetry data generated by the GG system, including overheads and margins, is 2350 Mbit/day (see §6.6). This amount of data may be downloaded on each ground station pass, once per orbit, minimizing the telemetry rate, or the number of contacts per day can be reduced in order to reduce Malindi ground station occupation time. The guideline for re-use of PRIMA hardware limits the TM symbol rate to 512 kbps, and leads to adoption of Reed-Solomon coding and SP-L modulation.

Assuming the data volume generated in one day of science operations must be downloaded within the next day, Table 6-9 shows, as function of number of contacts per day, the minimum TM data rate allowing data volume downlink. The values in red exceed the limit of 512 kbps, so they are not allowed.

Number of contacts/day	No data compression		Compression factor 1.5 (zip		Compression factor 2.8	
	TM data rate [kbps]	TM symbol rate [kb/s]	TM data rate [kbps]	TM symbol rate [kb/s]	TM data rate [kbps]	TM symbol rate [kb/s]
1 / orbit	263	300	175	200	94	107
10	392	447	261	298	140	159
9	435	496	290	331	155	177
8	490	558	326	372	175	199
7	560	638	373	425	200	228
6	653	744	435	496	233	266
5	783	893	522	595	280	319
4	979	1116	653	744	350	399
3	1306	1489	871	992	466	532
2	1959	2233	1306	1489	700	797
1	3917	4466	2612	2977	1399	1595

Table 6-9: TM data rates with limitation to 512 kbps

The conclusions from the table above are that:

- without data compression 9 contacts per day are necessary;
- with “zip file” technique (compression factor = 1.5) this number can be reduced to 6;
- using a Rice algorithm (compression factor = 2.8), 4 contacts per day are enough to download the whole mass memory content.

Link budget calculations have been performed for the worst case, i.e. no data compression, with and without ranging. With the architecture proposed, margins are such that ranging operations are guaranteed as well (Table 6-10). The TC link will be established at 4 kbps following the PCM/PSK/PM modulation scheme, according to standard ECSS-E-50-05A. Ranging too will be implemented in accordance with standard ECSS-E-50-02A.

Distance [km]	UP-LINK				DOWN-LINK						
	Data Rate [kbps]	Nom. Margin [dB]			Information Rate [kbps]	TM Coding	TM symbol rate [kbps]	Flux	Nom. Margin [dB]		
		RX power	Carrier Rec.	TC Recovery					Carrier Rec.	TM Recovery	Ranging
600	4	35.72	53.65	44.27	435	R-S	496	7.48	34.55	3.43	45.19
600	4	35.72	54.45	45.07	435	R-S	496	6.93	35.10	3.98	No RG

Table 6-10: Link budget summary

6.6 BUDGETS

6.6.1 MASS PROPERTIES

In the following, mass and inertia tables are provided, as follows.

- CoG, MoI and PoI budgets in Figure 6-17;
- GG Experiment mass budget in Table 6-11;
- GG Spacecraft Subsystems Mass Budget in Table 6-12;
- GG Spacecraft System Mass Budget in Table 6-13.

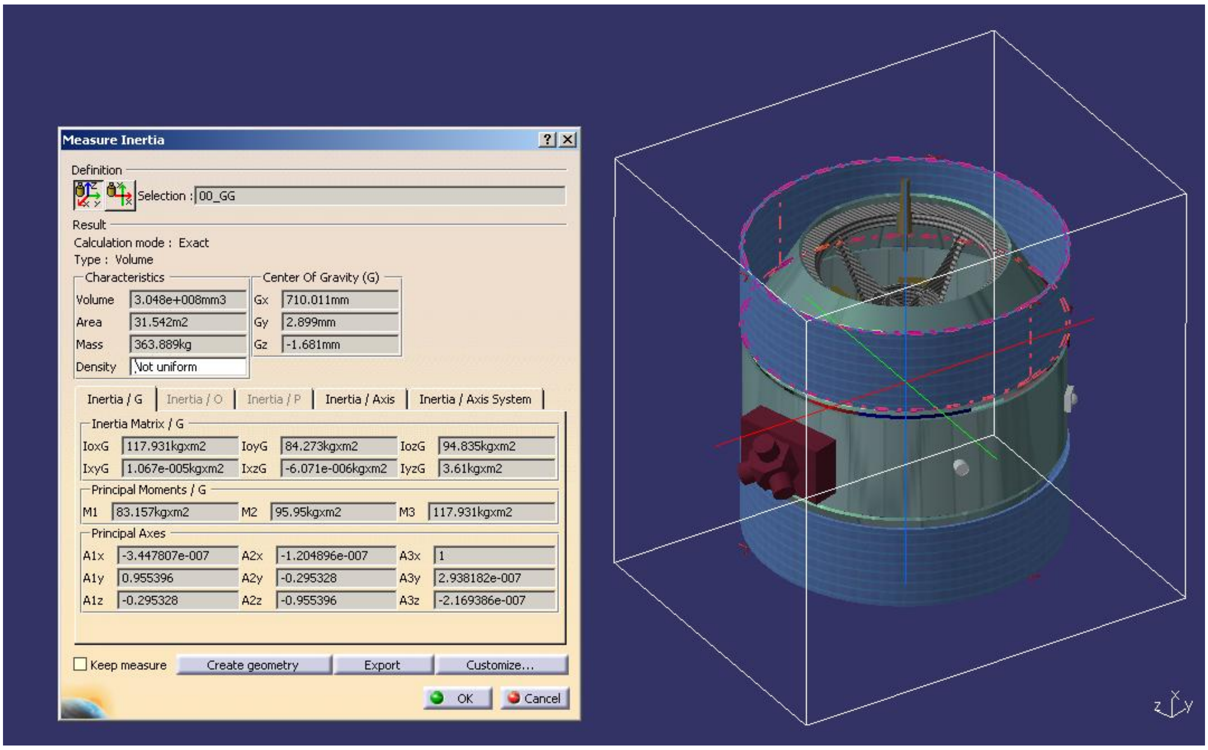

Figure 6-17: GG Spacecraft CoG, MoI and PoI budgets

Name	No.	Unit Mass [kg]	Total Mass [kg]	Margin [%]	Margin [kg]	Total Mass with margin [kg]
Inner Test Mass	**1**	**10,168**	**10,168**	**0**	**0,00**	**10,17**
Outer Test Mass	**1**	**10,183**	**10,183**	**0**	**0,00**	**10,18**
PGB Shaft			**2,879**	**20**	**0,58**	**3,45**
Mollette giunto 1	1	0,102	0,102			
Mollette giunto 2	1	0,071	0,071			
Mollette supporto piezo 1	1	0,098	0,098			
Mollette supporto piezo 2	1	0,030	0,03			
Assy supporto centrale	1	0,060	0,06			
Cilindro Giunto interno 1	1	0,161	0,161			
Cilindro Giunto interno 2	1	0,049	0,049			
Cilindro portante	1	1,082	1,082			
Piastre capacitive	1	1,164	1,164			
Piastrine capacitive	1	0,062	0,062			
PGB Shell allocation (TBC)	**1**	**7,60**	**7,60**	**20**	**1,52**	**9,12**
Locking mechanisms allocation (TBC)	**1**	**8,40**	**8,40**	**20**	**1,68**	**10,08**
Inch Worms allocation (TBC)	**12**	**0,10**	**1,20**	**20**	**0,24**	**1,44**
Thermal control allocation (TBC)	**1**	**3,00**	**3,00**	**20**	**0,60**	**3,60**
		PAYLOAD TOTALS	**43,43**	**10,6%**	**4,62**	**48,05**

Table 6-11: GG Experiment Mass Budget

Element 1 - Galileo Galilei						
FUNCTIONAL SUBSYSTEM	#	Mass (kg) per unit	Total Mass (kg)	Margin (%)	Margin (kg)	Mass (kg) with Margin
Structure			**102,11**	**20,00**	**20,42**	**122,53**
Upper Platform	1	1,23	1,23	20	0,25	1,48
Upper Cone	1	7,08	7,08	20	1,42	8,50
Outermost Cylinder	1	11,35	11,35	20	2,27	13,62
Lower Cone	1	7,08	7,08	20	1,42	8,50
Lower Platform	1	1,23	1,23	20	0,25	1,48
Cone to Cylinder I/F ring	2	14,58	29,16	20	5,83	34,99
Cone to Platform I/F ring	2	4,03	8,06	20	1,61	9,67
Lock/Unlock mechanism	2	2,50	5,00	20	1,00	6,00
Separation system ring	1	2,50	2,50	20	0,50	3,00
Miscellaneous (inserts. cleats. etc.	1	9,00	9,00	20	1,80	10,80
Mass Compensation System	1	7,50	7,50	20	1,50	9,00
Payload support cone	2	4,80	9,60	20	1,92	11,52
PGB interface	2	1,66	3,32	20	0,66	3,98
Thermal Control			**15,75**	**20,00**	**3,15**	**18,90**
S/C Thermal control allocation	1	15,75	15,75	20	3,15	18,90
Communications			**9,60**	**10,00**	**0,96**	**10,56**
XPDN S-Band 1	1	3,60	3,60	10	0,36	3,96
XPDN S-Band 2	1	3,60	3,60	10	0,36	3,96
RFDN S-Band	1	1,20	1,20	10	0,12	1,32
S-Band Antenna 1	1	0,60	0,60	10	0,06	0,66
S-Band Antenna 2	1	0,60	0,60	10	0,06	0,66
Data Handling			**16,00**	**20,00**	**3,20**	**19,20**
CTU+RTU	1	16,00	16,00	20	3,20	19,20
AOCS			**3,95**	**20,00**	**0,79**	**4,74**
Coarse Sun Sensor	1	0,65	0,65	20	0,13	0,78
Spin Rate Sensor	1	1,00	1,00	20	0,20	1,20
Earth Sensor	1	2,30	2,30	20	0,46	2,76
Propulsion			**33,50**	**13,32**	**4,46**	**37,96**
FEEP Thrusters	2	1,60	3,20	20	0,64	3,84
FEEP Electronics	2	5,60	11,20	20	2,24	13,44
Nitrogen Thrusters	6	0,10	0,60	5	0,03	0,63
Nitrogen Tank	2	7,16	14,32	5	0,72	15,04
Lines & Valves	1	1,80	1,80	20	0,36	2,16
FEEP Neutralizer	2	0,12	0,24	20	0,05	0,29
FEEP Miscellanea	1	2,14	2,14	20	0,43	2,57
Power			**34,40**	**12,88**	**4,43**	**38,83**
Solar Array	2	4,95	9,90	20	1,98	11,88
PCDU	1	20,00	20,00	10	2,00	22,00
Battery	1	4,50	4,50	10	0,45	4,95
Harness			**12,50**	**20,00**	**2,50**	**15,00**
Harness	1	12,50	12,50	20	2,50	15,00
Payload			**56,03**	**12,74**	**7,14**	**63,17**
Inner test mass	1	10,17	10,17	0	0,00	10,17
Outer test mass	1	10,18	10,18	0	0,00	10,18
PGB Shaft	1	2,88	2,88	20	0,58	3,45
PGB Shell allocation	1	7,60	7,60	20	1,52	9,12
ECE	1	5,40	5,40	20	1,08	6,48
CPE	1	7,20	7,20	20	1,44	8,64
Locking Mechanisms allocation	1	8,40	8,40	20	1,68	10,08
Inch Worms allocation	12	0,10	1,20	20	0,24	1,44
P/L Thermal Control allocation	1	3,00	3,00	20	0,60	3,60
Propellant						**3,75**

Table 6-12: GG Spacecraft Subsystems Mass Budget

Galileo Galilei						
		Target Spacecraft Mass at Launch			1000,00	kg
		Below Mass Target by:			535,43	kg
	Without Margin		Margin		Total	% of Total
Dry mass contributions			%	kg	kg	
Structure	**102,11 kg**		**20,00**	20,42	**122,53**	26,38
Thermal Control	**15,75 kg**		**20,00**	3,15	**18,90**	4,07
Communications	**9,60 kg**		**10,00**	0,96	**10,56**	2,27
Data Handling	**16,00 kg**		**20,00**	3,20	**19,20**	4,13
AOCS	**3,95 kg**		**20,00**	0,79	**4,74**	1,02
Propulsion	**33,50 kg**		**13,32**	4,46	**37,96**	8,17
Power	**34,40 kg**		**12,88**	4,43	**38,83**	8,36
Harness	**12,50 kg**		**20,00**	2,50	**15,00**	3,23
Payload	**56,03 kg**		**12,74**	7,14	**63,17**	13,60
Total Dry(excl.adapter)	**283,84**				**330,89 kg**	
System margin (excl.adapter)			**20,00 %**		**66,18 kg**	
Total Dry with margin (excl.adapter)					**397,07 kg**	
Other contributions						
Wet mass contributions						
Propellant	**3,75 kg**		**100,00**	3,75	**7,50**	1,61
Adapter mass (including sep. mech.), kg	**60,00 kg**		**0,00**	0,00	**60,00**	0,13
Total wet mass (excl.adapter)					**404,57 kg**	
Launch mass (including adapter)					**464,57 kg**	

Table 6-13: GG Spacecraft System Mass Budget

6.6.2 POWER BUDGETS

The power demand of the satellite is about 519 W including maturity margins and a system margin of 20%, as reported in Table 6-14.

Equipments	No.	Power [W]	Contingency [%]	Contingency [W]	Nominal Power [W]
ECE	1	9,12	20%	2,28	11.40
CPE	1	18,4	20%	4,6	23.00
Total P/L					**34.40**
Spacecraft Management Unit	1	18	10%	1,8	19.8
Transponder 1 (TX & RX)	1	20	10%	2	22
Transponder 2 (RX)	1	6	10%	0.6	6.6
PCDU	1	20	10%	2,00	22
Battery (max charging)	0	180	-	-	190
TCS Heaters	1	40	20%	8	48
Coarse Sun Sensor	1	0.5	10%	0.1	0.6
Earth & Sun Sensor	1	6	10%	1.2	7.2
Harness loss + PCDU loss	1	20	20%	4	22
FEEP Electronics (assuming an thrust average of 300 uN)	1	100	10%	10	60
Total Service Module					**398.2**
Total Satellite					**432.60**
System margin			**20%**		**86.52**
G R A N D T O T A L					**519.12**

Table 6-14: Satellite power demand

6.6.3 Data budgets

The mass memory budget and hence the telemetry data rates depend on the data collection mode. The total science data rate in the normal scientific mode is about 158 Mbit/orbit including all overheads and margins (Table 6-15).

An on board mass memory sized for 24-hour autonomy would amount to about 1.6 Gbit. The whole 24-hour memory contents could be downloaded to the ground station in one single pass of 10’ duration at a rate of about 186 kbps that is compatible with the maximum data rate permitted by the ESA S-band stations.

Data description	Variable list	Number of variables	Freq. [Hz]	Record length [bit]	Data rate [kbit/s]
Diff. TMs displacement	Δx, Δy	2	50	16	1.6
Tme/PGB displacement	Δx, Δy, Δz	3	50	16	2.4
Tmi/PGB displacement	Δx, Δy, Δz	3	50	16	2.4
PGB/Spacecraft displac.	Δx, Δy, Δz	3	50	16	2.4
ω_{SPIN}	ω_x, ω_y, ω_z	3	50	16	2.4
Reference time	t	1	50	16	0.8
Science data					**12.0**
PGB whirl monitoring	Sensing + actuation	6	1	16	0.096
Tme whirl monitoring	Sensing + actuation	6	1	16	0.096
Tmi whirl monitoring	Sensing + actuation	6	1	16	0.096
ADC monitoring	Number of ADC	9	1	16	0.144
Inchworm monitoring	Number of inchworms	6	1	16	0.096
Piezo monitoring	Number of piezo	6	1	16	0.096
PGB Inner temperature monitoring	Number of temperature sensors	20	0.10	16	0.03
Capacitance bridge monitoring	Number of capacitance bridges	9	0.10	16	0.01
Payload HK					**0.7**
Commands to FEEP	Number of commands	6	1	16	0.096
PGB/Spacecraft phase lag	Number of lag sensors	1	0.10	16	0.0016
Commands to actuators	Number of commands	6	50	16	4.8
Sun sensor	1 (2 in case o redundancy)	2	50	16	1.6
FEEP monitoring	Number of FEEP	6	1	16	0.096
SVM (DFACS + other sub-systems)					**10.0**
			Total Data Rate	kbps	**22.7**
			Overhead		**20.0%**
			Total Data Rate with margins	kbps	**27.2**
			Altitude	km	**600**
			Period	s	**5801**
			Data volume	Mbit/orbit	**158**
			Pass duration	minutes	**10**
			Telemetry rate	kbit/s	**263**
			Passages/day		**14**
			Telemetry data volume	Mbit/day	**2350**

Table 6-15: Satellite data budgets